

# A Complete Model for Iron Losses Prediction in Electric Machines Including Material Measurement, Data Fitting, FE Computation and Experimental Validation

**Abstract.** This paper presents a complete model & process for predicting the iron losses in electric machines. The method includes material measurement, data fitting for loss coefficient determination, FE computation and experimental validation. The model is based on the loss separation of hysteresis and eddy-current losses. Also a least squares based method of curve fitting, to obtain material loss coefficients for FE analysis, is derived from the tested specific core losses of a steel lamination ring sample. The generality of the completed method is further verified by application to different steel types and electric machines. The results predicted by the model show excellent agreement with the tested data for a high speed PM DC motor and a PM BLDC motor.

**Streszczenie.** Zaprezentowano metodę przewidywania strat w maszynach elektrycznych uwzględniając właściwości materiałowe, współczynniki strat, obliczenia numeryczne i weryfikację eksperymentalną. (Model strat w żelazie w zastosowaniu do przewidywania strat w maszynach elektrycznych)

**Keywords:** Electric machines, finite element analysis (FEA), iron losses, laminated steel, motors.

**Słowa kluczowe:** maszyny elektryczne, straty, metoda elementów skończonych.

## Introduction

It is necessary for electrical machine designers to be able to accurately predict iron losses, particularly in the development of premium electric motors & generators. As a result, the topic of iron losses prediction in electric machines is always an intensely researched area. The first widely accepted iron losses model was the Steinmetz model which is composed of two constant coefficients [1]. Later Bertotti introduced a three constant coefficient model which has become one of the widely accepted models [2]. In this model the iron losses are separated into three parts, hysteresis loss, eddy current loss and excess loss which represented an improvement over the original. More recently there has been some two and three variable coefficient models introduced [3-6]. However due to the complex nature of the problem the accuracy and range of application of all iron losses models such as these has remained a challenge. The accumulated error in the process of iron losses computation may, in some cases, reach as high as 30% [3]. To date the search continues for models that can reasonable predict iron losses across a wide range of machines.

The aim of this paper is to present a model and a process for iron losses prediction in electric machines, in which the material measurement, data fitting for loss coefficients, FE computation and experimental validation, are included completely. In this model the material loss description is based upon a traditional two terms formulation. The coefficients used here are variable, simply determined and particularly suited for electric machine iron losses prediction. Finally, the predicted results are compared with actual iron losses experimental test data for two different motors. The predicted iron losses agree well with the experimental ones.

## Material Measurement

### A. Test Bench Description

To begin the test procedure, the lamination core ring, as shown in Fig. 1, is selected with the following specifications.

1) Lamination cut into a ring measuring: 65 mm O.D., 45 mm I.D., and a stack length of up to 10-11mm high.

2) Measure the height of the stack in 0.01 mm increments while exerting 20 kg of pressure on the stack.

3) Weigh the net weight of the stack in 0.1 gram increments.

Further, the Brockhaus Messtechnik MPG 100D & MPG Expert DC/AC model is adopted for testing the losses, the test bench used is shown in Fig. 2. The main characteristics of the measurement system are as follows:

- 1) High accuracy and repeatability.
- 2) Actively controlled sinusoidal flux density waveform.
- 3) Large scale field strength and polarization.

### B. Measured Specific Core Losses

The specific core losses of sample steel A and B were measured and the characteristics are shown in Table I while the measured losses are shown in Fig. 3(a) and (b).

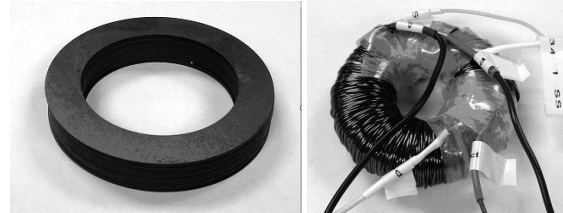


Fig. 1. Appearance of measured steel lamination ring core and coils

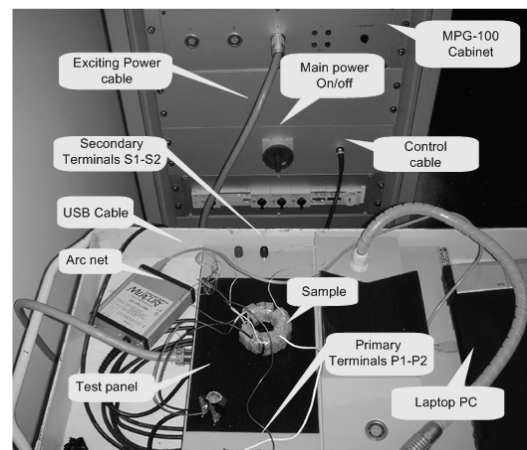


Fig. 2. Test Bench for the special core losses

Table 1 Details of the Lamination Steels

Material Type	Ste	
	el A	el B
Thickness (mm)	0.5	0.5
Conductivity (s/m)	2.5	2.5
Flux density at 5000A/m (T)	$\times 10^6$ 1.6	$\times 10^6$ 1.6
Core loss at 1.5 T&50Hz (W/kg)	3	1
	65	4.1
Fully processed	Yes	Yes

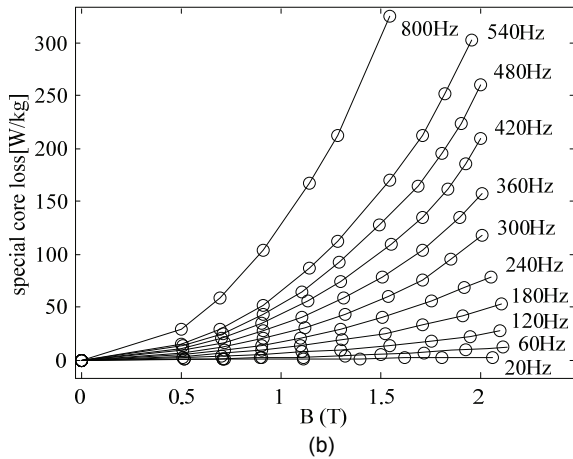
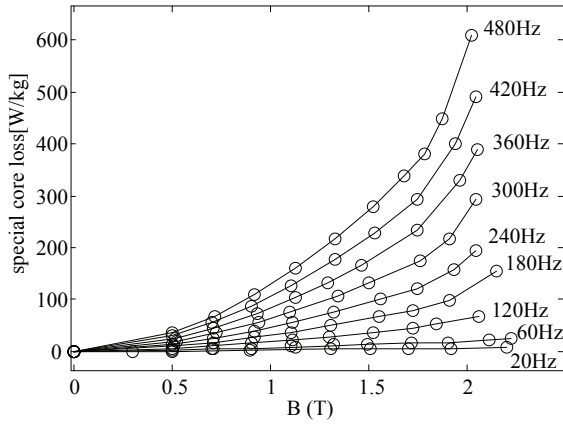


Fig.3. Measured specific core losses of sample steels. (a) Steel A. (b) Steel B.

### Iron Loss Model Description

#### A. Model Description

It is widely known that iron losses can be separated into two main terms, eddy current and hysteresis losses in (1):

$$(1) \quad W_{fe} = \sigma f B^\alpha + \varepsilon (fB)^2$$

In (1),  $f$  is the frequency of the magnetic field,  $B$  is the flux density,  $\sigma$  is the hysteresis loss coefficient,  $\alpha$  is the Steinmetz coefficient and  $\varepsilon$  is the eddy-current loss coefficient. Equation (1) can be transformed to (2):

$$(2) \quad W_{fe} = Y_{(B_p)} f + K_{(B_p)} f^2$$

Dividing (2) by  $f$ , the formulation becomes a simple first-order polynomial with the following form.

$$(3) \quad \frac{W_{fe}}{f} = Y_{(B_p)} + K_{(B_p)} f$$

In (3),  $Y_{(B_p)}$  is the hysteresis loss coefficient and  $K_{(B_p)}$  is the eddy current coefficient. Obviously, it is a simpler model since the coefficients  $K$  and  $Y$  depend only upon the flux density peak  $B_p$ , which can be obtained from the measured special core losses by the least squares method.

#### B. Loss Coefficients Determination

The loss coefficients can be determined by the least-squares method using a first-order polynomial. For the two types of steels above, the coefficients are given in Fig.4 and Fig.5.

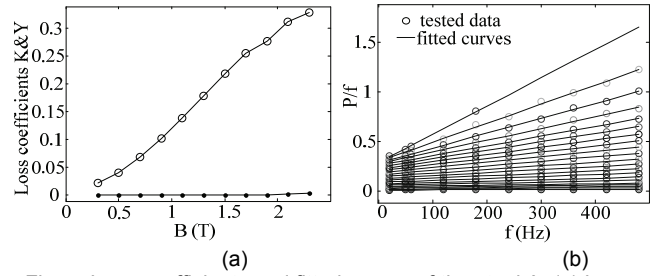


Fig. 4. Loss coefficients and fitted curves of the steel A. (a) Loss coefficients K&Y. (b) Comparison of tested and fitted loss data.

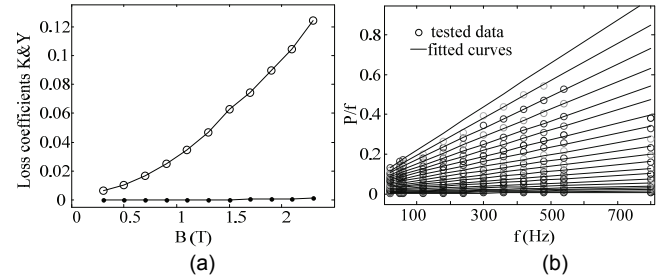


Fig. 5. Loss coefficients and fitted curves of the steel B. (a) Loss coefficients K&Y. (b) Comparison of tested and fitted loss data.

#### C. Characteristics of the Model

According to the above description, loss coefficient determination, the main characteristics of this new model can be summarized as follows.

1) Compared to other recent formulations, this new model requires only two coefficients to be determined, namely  $K$  and  $Y$ . Furthermore both  $K$  and  $Y$  are functions of the peak of the amplitude of the flux density  $B_p$ .

2) The coefficients  $K$  and  $Y$  vary with the frequency of the supplied field and the amplitude of the flux density. Close comparison of Fig. 4(b) and Fig. 5(b) show that the fitted curves show a good agreement with the tested data.

3) It is not necessary to perform a complex mathematical procedure to obtain these coefficients.

### The Difference In Iron Losses Prediction Between Lamination Steel and Actual Electric Machines

Based on the improved model in section III, the losses of lamination steel material can be predicted directly and accurately. However, there are important distinctions between the iron losses prediction in lamination steel material and iron losses prediction in electric machines. The predicted losses in electric machines are sometimes very different from actual test, when the loss computation is based only on direct use of the material curves. The reasons stem from some specific factors related to electric machines such as uneven flux density distribution, the harmonic nature of the field and the rotational nature of the field. There continues to be a lack of generic methods to address these problems. In this section, these special problems are analyzed and various techniques are employed, so that a more complete iron losses prediction can be performed.

#### A. Uneven Flux Density Distribution

The flux density distribution in the sample steel is even when the test bench, shown in Fig. 2, is used for measuring the specific core losses, however it is uneven in a motor core [7]. Fortunately, the flux density at any location within an iron core of motor can be easily computed by FEA.

### B. Harmonic Field

The iron losses model presented in section III is derived for the simple sinusoidal excitation condition however in the case of a motor core the situation is not this simple. There is the interaction of the fundamental and harmonic fields, especially in the area of the surface of the stator and rotor. Therefore, it is necessary to consider the contribution to the total losses from the harmonic field even though the amplitudes of these components are typically very low and do not saturate the core. To account for these effects, a correction factor is used when considering the harmonic field with reference to [8]. Specifically we utilize a factor of 60% on the amplitude of the harmonic flux density as a correction. This flux density waveform is the result of a magnetostatic FEA solution at successive rotor positions.

### C. Rotational Field

The rotational field's contribution to the total losses is often computed by using one or more of the following techniques. The first is to take into account the independent orthogonal components, in which both the radial and tangential components are computed. The total losses then are estimated by summing up the losses produced by the two orthogonal components [9]. The second method is to utilize correction factors, in which the relative factors are applied to account for the variation in the peak of the flux density as well as the rotational field [10-11]. Lastly, the vector hysteresis approach is also used to account for the influence of hysteresis on the magnetic flux distribution inside a motor [11]. After analyzing a large amount of computed iron losses data and trying to manage the overall complexity of the resultant model the first method was chosen for the iron losses model presented in this paper.

### Computational Results and Experimental Validation

Two different kinds of motors, a high speed PM DC motor and a PM BLDC motor, are used for experimental validation. Details of the motors are given in Table 2. The spin test rig with a test motor mounted is shown in Fig.6. The tests are carried out with and without permanent magnet and the difference in measured mechanical power required to spin the motors is the result of the iron losses.

#### A. Experimental Validation of the High Speed PM DC Motor

The tested and computed iron losses of a high speed PM DC motor, within the speed range from 5000 rpm to 25000 rpm, is shown in Fig. 7. As seen in the figure, the computed losses show very good agreement with the tested ones. Additionally, the loss density distribution is given in Fig.8(a) 5000 rpm, 83.33 Hz and 8(b) 25000 rpm, 333.33 Hz. From these figures one can clearly see that:

- 1) The loss density at higher frequencies and speeds is much higher. The local maximum loss density at 25000 rpm and 333.33 Hz reaches 500 W/kg, which is nearly 10 times higher than that at 5000 rpm and 83.33 Hz.
- 2) The example PM DC motor carries very high loss density in the rotor tooth body under high speed operation. Upon analyzing the computed flux density distribution of the motor, it can be seen that the peak of the flux density in tooth is above 1.8 T, which indicates very high saturation levels in this area of the motor.

Table 2 Details of the Two Sample Motors

Motor	PM DC	BLDC
Output(W)	400	250
Poles	2	4
Steel type	A	B
Stator outer diameter (mm)	47	75
Stator inner diameter (mm)	35.45	37
Core-length (mm)	30	10

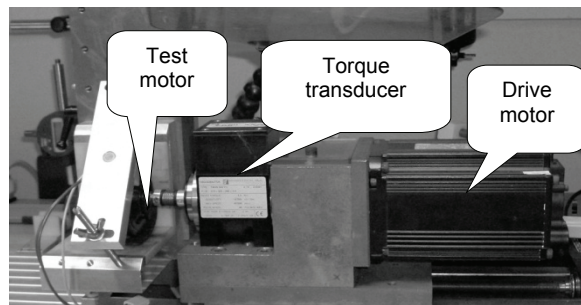


Fig. 6. The picture of the spin test rig

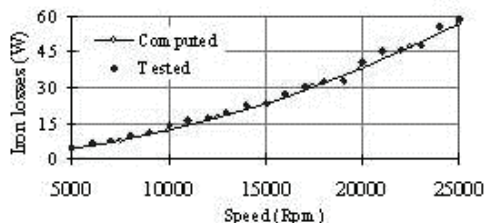


Fig. 7. Comparison of tested and computed iron losses of PM DC motor

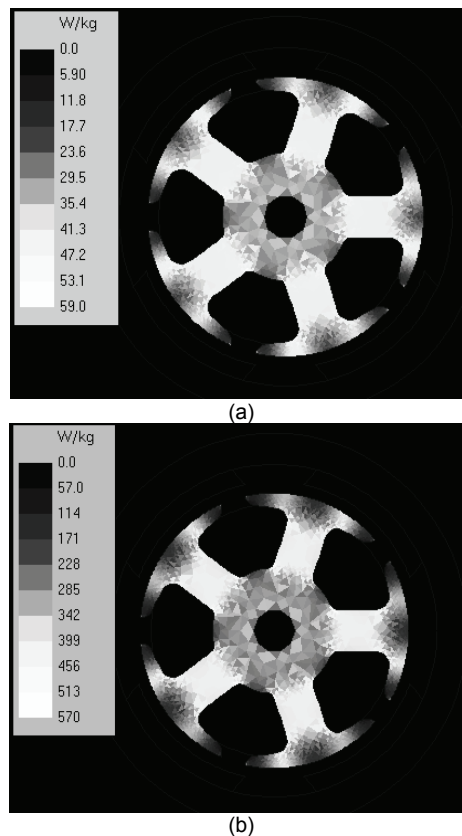


Fig. 8. Loss density distribution of the PM DC motor. (a) At 5000 rpm, 83.33 Hz. (b) At 20000 rpm and 333.33 Hz.

#### B. Experimental Validation of the PM BLDC Motor

The tested and computed iron losses of the PM BLDC motor, within the speed range of 2500 rpm to 20000 rpm, is shown in Fig. 9, and the computed losses show very good agreement with the tested ones. The loss density distribution is given in Fig.10 (a) 2500 rpm, 83.33 Hz and Fig.10 (b) 20000 rpm, 666.66 Hz. It can be seen that:

- 1) The same relationship between loss density and speed is exhibited in the PM BLDC as in the PM DC motor of the Fig.7 and Fig. 8.
- 2) Unlike the example high speed PM DC motor, the PM BLDC motor concentrates its losses in the top of the stator tooth area. This reflects the inherent structural difference

between motor types. Additionally, the two motors have very different saturation levels, which severely influence their loss densities, 1.4 T vs. over 1.8 T.

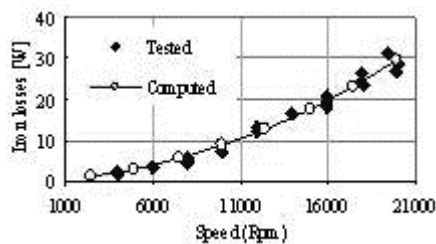


Fig. 9. Comparison of tested and computed iron losses of the PM BLDC motor

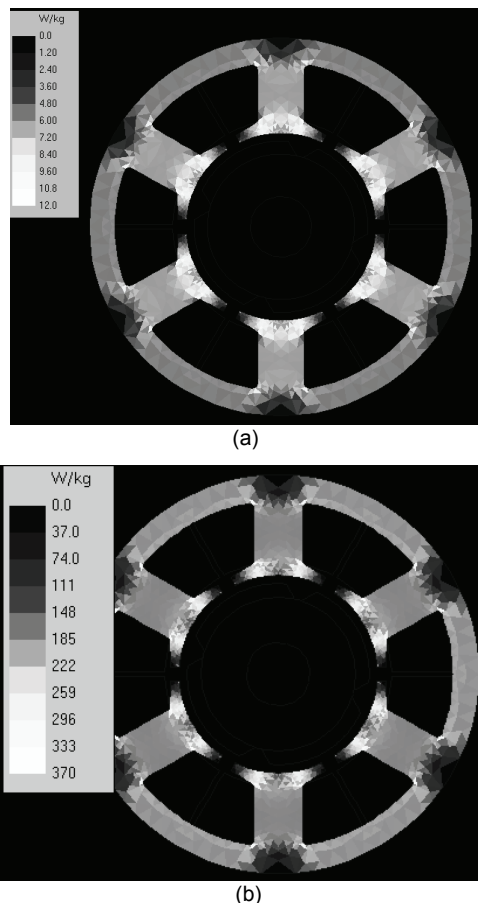


Fig. 10. Loss density distribution of the PM BLDC motor. (a) At 2500 rpm and 83.33 Hz. (b) At 20000 rpm and 666.66 Hz

## Conclusions

A complete model for predicting iron losses, including material measurement, data fitting, FE computation and experimental validation, has been proposed. The model is convenient to use and able to predict the iron losses of electric machines with good accuracy. The model's results and therefore its utility have been verified by comparison with test data.

## Acknowledgments

This work is supported in part by the Fundamental Research Funds for the Central Universities.

## REFERENCES

- [1] C.P. Steinmetz, On the law of hysteresis (originally published in 1892), *Proc. IEEE*, 72 (1984), no. 2, 196-221
- [2] Giorgio Bertotti, General properties of power losses in soft ferromagnetic material, *IEEE Trans. Magn.*, 24 (1988), no. 1, 621-630
- [3] Mircea Popescu, Dan.M. Ionel, A Best-Fit Model of Power Losses in Cold Rolled-Motor Lamination Steel Operating in a Wide Range of Frequency and Magnetization, *IEEE Trans. Magn.*, 43 (2007), no. 4, 1753-7756
- [4] Jian Guo Zhu, Victor Stuart Ramsden, Improved Formulations for Rotational Core Losses in Rotating Electrical Machines, *IEEE Trans. Magn.*, 34 (1998), no. 3, 2234-2242
- [5] Lotten Tsakani Mthombeni, Pragasen Pillay, Core Losses in Motor Laminations Exposed to High-Frequency or Nonsinusoidal Excitation, *IEEE Trans. Ind. Applicat.*, 40 (2004), no. 5, 1325-1332
- [6] Katsumi Yamazaki, Noriaki Fukushima, Iron-Loss Modeling for Rotating Machines: Comparison Between Bertotti's Three-Term Expression and 3-D Eddy-Current Analysis, *IEEE Trans. Magn.*, 46 (2010), no. 8, 3121-3124
- [7] S. O. Kwon, J. J. Lee, B. H. Lee, K. H. Ha, J. P. Hong, Loss distribution of three-phase Induction motor and BLDC motor according to core materials and operating, *IEEE Trans. Magn.*, 45, (2009), no. 10, 4740- 4743
- [8] J. D. Lavers, P. P. Biringer, H. Hollitscher, A simple method of estimating the minor loop hysteresis loss in thin lamination, *IEEE Trans. Magn.*, 14 (1978), no. 5, 386-388
- [9] Guzmán Díaz, Cristina González-Morán, Pablo Arbolea, Javier Gómez-Aleixandre, "Analytical interpretation and quantification of rotational losses in stator cores of induction motors" *IEEE Trans. Magn.*, 43 (2007), no. 10, 3861-3867
- [10] Carlos A. Hernandez-Aramburo, Tim C. Green, Alexander C. Smith, "Estimating Rotational Iron Losses in an Induction Machine," *IEEE Trans. Magn.*, 39 (2003), no. 6, 3527-3533
- [11] Oriano Bottauscio, Aldo Canova, Mario Chiampi, Maurizio Repetto, "Iron Losses in Electrical Machines: Influence of Different Material Models," *IEEE Trans. Magn.*, 38 (2002), no. 2, 805-808.

## Authors

Corresponding author: Zhao Haisen, School of Electrical and Electronic Engineering, North China Electric Power University.

Address: No. 2 Beinong Road, Hui Longguan, Changping District, Beijing, 102206, P.R. China  
[zhaohaisen@163.com](mailto:zhaohaisen@163.com) for Zhao Haisen;